Experimental and Numerical Analysis on a Thermal Barrier Coating with Nano-Ceramic Base: A Potential Solution to Reduce Urban Heat Islands?

Bruno Malet-Damour, Dimitri Bigot, Garry Riviere

eng

MDPI

Article

Experimental and Numerical Analysis on a Thermal Barrier Coating with Nano-Ceramic Base: A Potential Solution to Reduce Urban Heat Islands?

Bruno Malet-Damour *, Dimitri Bigot and Garry Rivière

PIMENT Laboratory, University of Reunion Island, 120 Avenue Raymond BARRE, 97430 Le Tampon, Reunion Island, France; dimitri.bigot@univ-reunion.fr (D.B.); garry.riviere@univ-reunion.fr (G.R.)
* Correspondence: bruno.malet-damour@univ-reunion.fr

Abstract: Adopting a multiscale approach is crucial for optimizing urban and building performance, prompting inquiries about the link between a technology's local efficiency (building scale) and its broader impact (city-wide). To investigate this correlation and devise effective strategies for enhancing building and city energy performance, we experimentally examined a commercial nano-ceramic Thermal Barrier Coating (TBC) on a small-scale building and assessed numerically its influence on mitigating Urban Heat Islands (UHIs) at a city scale, translated in our case by the use of the thermal comfort index: the Universal Thermal Climate Index (UTCI). Our results reveal that the coating significantly curbs heat transfer locally, reducing surface temperatures by over 50 °C compared to traditional roofs and attenuating more than 70% of heat flux, potentially alleviating air conditioning demands and associated urban heat effects. However, implementing such coatings across a city does not notably advance overall efficiency and might trigger minor overheating on thermal perception. Hence, while nano-ceramic coatings indirectly aid UHI mitigation, they are not a standalone fix; instead, an integrated strategy involving efficient coatings, sustainable urban planning, and increased vegetation emerges as the optimal path toward creating enduringly sustainable, pleasant, and efficient urban environments to counter urban heat challenges effectively.

Keywords: Thermal Barrier Coating—TBC; experimental analysis; numerical analysis; UHI; UTCI; building performance

Citation: Malet-Damour, B.; Bigot, D.; Rivière, G. Experimental and Numerical Analysis on a Thermal Barrier Coating with Nano-Ceramic Base: A Potential Solution to Reduce Urban Heat Islands? *Eng* **2023**, *4*, 2421–2442. https://doi.org/10.3390/eng4030138

Academic Editors: George Z. Papageorgiou, Maria Founti and George N. Nikolaidis

Received: 13 July 2023
Revised: 31 August 2023
Accepted: 15 September 2023
Published: 19 September 2023

1. Introduction

An Urban Heat Island (UHI) refers to areas where temperatures are significantly higher within urban environments than adjacent rural areas. This phenomenon primarily arises from the accumulation of heat generated by human activities (air conditioning systems, industry, transport, etc.), the density of built spaces, the alteration of natural landscape elements, and thermal absorption by urban surfaces, like roads and buildings. UHIs are exacerbated by heat waves rising due to climate change.

Both buildings (at the local scale) and cities (at the global scale) must develop tangible and practical solutions to ensure indoor and outdoor comfort for individuals. Hence, it is essential to establish a close relationship between building design and urban planning, as the design of one naturally influences the other.

At the local scale, the critical role of a building's envelope in occupants' thermal comfort lies in its ability to ensure optimal energy performance. For decades, insulation has been promoted to shield building interiors from external environmental influences, thereby reducing heat transfer and the need for energy-intensive active systems to regulate indoor thermal conditions. Solar irradiation can reach high values in regions with warm and tropical climates, such as Reunion Island, even up to 1200 W.m^{-2}. This solar influx results in significant heat gains within structures. Solar radiation on rooftops can contribute up to 50% of the total building's thermal load in such warm contexts [1]. These heat transfers

are exacerbated by construction errors, mainly causing thermal bridges, and by dense and poorly planned urban environments.

Installing air conditioning systems in inadequately designed constructions will inevitably impact the release of heat energy into the external environment. However, simple solutions, such as altering surface colors and using highly reflective thermal materials, pay homage to traditional practices reminiscent of certain Greek islands, like Santorini. The mere application of white paint increases wall reflectivity, limiting heat absorption. A material can achieve high emissivity by incorporating, for example, ceramic properties while maintaining low absorptivity and transmittance. These technologies, frequently referred to as Thermal Barrier Coatings (TBC), could potentially significantly enhance building efficiency and positively impact Urban Heat Island phenomena on a broader scale.

However, the capacity of a single coating solution to perform effectively at various scales has yet to be demonstrated. Therefore, in this article, we introduce two distinct approaches (experimental and numerical) to address the following question: Can Thermal Barrier Coatings simultaneously enhance building energy efficiency and mitigate the effects of Urban Heat Islands on a city-wide scale considering their impact on thermal comfort?

The fundamental objective of this article is to provide a multiscale analysis of the performance of a nano-ceramic-based TBC. This analysis is conducted through experimental studies (at the building scale) and numerical simulations (at the city scale). Our approach focuses on a commercially available coating (by Thermacote®), grounding our evaluation in factual properties rather than theoretical assumptions.

Initially, we will offer a brief overview of the current state of knowledge regarding the application of Thermal Barrier Coatings in construction, highlighting the lack of consensus in terminology. Within this context, we will examine research that has investigated using these coatings at an urban scale to alleviate Urban Heat Island effects. Subsequently, we will present our experimental and numerical methodological approaches and their goals. Finally, we will discuss the findings.

This experimental study aims to compare the effectiveness of this coating with commonly employed construction methods in warm and tropical climates, particularly on Reunion Island. To achieve this, we subjected a scaled-down building model (at a 1:14 scale) to artificial solar exposure, enabling an assessment of the impact of the nano-ceramic-based TBC under various scenarios and conditions.

Building upon observations made at the local scale (building level), we then analyzed the impact of this type of TBC at the city scale. This numerical analysis seeks to validate the solution's effectiveness on a broader scale (urban level). It provides insights into its potential to alleviate Urban Heat Island effects by acting on external thermal comfort. This is translated through utilizing a comfort indicator, the Universal Thermal Climate Index (UTCI). These multiscale approaches will enable us to evaluate a singular technical solution's efficacy comprehensively.

2. Overview of Advancements in TBCs for Building Applications

From the latest state of the art in this field, most research focuses on the chemical designing of the best Thermal Barrier Coating (TBC) to achieve the best mechanical, thermal, environmental, and durability performances [2–7]. The research goals are often to better understand the development or fabrication process of TBC materials or to improve their performances for high temperatures, with the most current applications being gas turbines or automobile coatings [8–24]. Liu et al. [11] listed the five principal nanomaterial classes used to make TBCs and described their characteristics and preparation methods [11]: oxides, perovskites, pyrochlores, magnetoplumbites, and high-entropy ceramics. They compared the preparation methods and presented an analysis of their failure mechanisms as residual stresses, sintering failure, erosion and corrosion cracking, and thermally-grown oxide (TGO) growth. Their work completed the works of Vaßen et al. [25], made in 2010, that concludes on the interest of developing the multilayer TBC concept [25]. They also proposed performance improvement strategies for hardness, fracture toughness and

tribological properties, thermal conductivity, thermal expansion coefficient, thermal cycling life, thermal shock life, and hot corrosion behavior. Their strategies were set up for single-layer coatings and multilayer ones. Focusing on the subject of labor addressed in this present article, it is noteworthy that the authors have omitted references to building-related applications, instead focusing solely on high-temperature applications. This observation implies that analogous studies should be conducted to assess the performance of TBCs in construction-oriented applications, especially when confronted with humidity constraints.

Directing our focus to the realm of construction, numerous investigations have been undertaken concerning the utilization of Thermal Barrier Coatings (TBCs) on building walls. These endeavors aim to ameliorate issues of excessive heat accumulation or unwarranted cooling, ultimately enhancing the energy efficiency of buildings. This scholarly exploration encompasses comprehensive literature analyses [26–29]. Within the literature, three distinct technological avenues have garnered recurrent mention: reflective coatings, low-emissivity coatings, and a combination of the two. The first approach physically reflects incident energy, the second curtails the energy emission from the underlying wall structure, and the third amalgamates both effects.

At this stage, making a physical definition focus on these terminologies is interesting. Indeed, high reflectivity means low absorptivity due to the relation between absorptivity, reflectivity, and transmissivity: $\alpha + \rho + \tau = 1$ (with $\tau = 0$ for an opaque body) [30]. Furthermore, one can notice that low thermal emissivity often goes hand in hand with low thermal absorptivity for many common building materials, although this is not a guarantee. It is essential to correctly understand this because these materials are often described as good thermal insulators.

For example, Bozsaky [31] tried to measure the thermal conductivity of some TBCs [31,32] with the same methodologies as insulation material ones. He found that conventional methods, such as heat flux and hot box, are challenging to apply to coatings due to their low thicknesses. He found thermal conductivities near the ones of traditional insulation materials and concluded that one has to be careful before saying a TBC is a good insulation material. Indeed, TBCs are often described as good thermal insulators, but it is more accurate to describe them as reflective or high emissive materials, as their main thermal properties are radiative.

TBC studies, for building applications, can mainly be classed into two parts: experimental and numerical. Experimental ones mainly compare TBCs with traditional coatings or other insulation systems, with the aim of reducing building energy needs or improving indoor thermal comfort [33–37]. Simulations focus on evaluating building energy savings or optimizing building envelope design to improve user comfort and decrease energy consumption [38–46].

The experimental and numerical results could be summarized as follows:

- TBCs are often called “cool paints” in UHI papers and as reflective coatings even if some high emissive properties are mentioned;
- Reflective paints are more efficient for avoiding solar energy absorption and reducing wall surface temperatures, with higher solar reflectances [33–35,45];
- Reflective paints can reduce inside air temperature in summer and increase it in winter, and so on, to be closer to the inside comfort temperature [35,38–44];
- TBCs, in most cases, reduce building energy needs for cooling and heating by reducing thermal losses through the walls [38–44];
- Radiation heat transfer is the dominant mechanism in the thermal modeling of TBCs [38–43];
- Reflective paints can lead to an increase in heating needs in winter, contrary to a reduction in cooling needs in the summer [35,47];
- A TBC with high solar reflectance and low emissivity should be a good candidate as a cool roof by reducing the wall U value [36,37];
- The TBC has to be placed outside the wall to be the most effective [38];

- TBCs are good candidates in building renovation cases for not enough insulated walls to reduce energy needs (R-values less than 1 $m^2.K^{-1}.W^{-1}$) [44];
- TBCs are more interesting when installed on roofs than in addition to vertical walls [48] because its impact is more significant there.

2.1. Proposed Terminology

Many studies have investigated Thermal Barrier Coatings from their reflective properties' point of view, and we have described above the confusion that can occur when many terminologies are used for the same phenomena. What can be drawn from all these studies is the need to improve further the phenomenological description of the heat transfers that take place in the walls of the building and to better characterize the thermo-physical properties of the materials used as a barrier.

Indeed, for example, another way to limit heat transfer due to solar irradiation through the building wall is to increase its exterior emissivity combined with a high thermal resistance through the wall. This field has not been explored as such. Some studies show such phenomena in their results but are not analyzed as such [28,36,37,46,49–51]. In some cases, a combination of relatively high emissivity and sufficient thermal resistance can lead to interesting results in the absorption and transmission of solar irradiation through the building wall. Indeed, in such cases, solar irradiation can be absorbed by a thin layer near the exterior surface of the wall. If its thermal resistance is sufficient, the thermal equilibrium leads to heat dissipation toward the environment by radiative emissions.

The previous authors were not interested in precisely describing the materials' radiative properties or did not want to, maybe for patentability reasons.

It would, therefore, seem attractive for the scientific community to clarify and systematize the classification of TBCs into three categories:

- A High-Reflective and Low-Emissive TBC: "HR-LE-TBC";
- A High-Emissive and Low-Reflective TBC with insulation: "HE-LR-TBC";
- A combination of these two radiative properties, a High-Emissive and High-Reflective TBC: "HE-HR-TBC".

It is important to note that thermal emissivity and solar reflectance are distinct optical properties, and achieving both high emissivity and high reflectance across a wide range of wavelengths can be challenging. Materials with high thermal emissivity tend to have lower solar reflectance and vice versa. However, the surface roughness can influence the properties of thermal emissivity and solar reflectance. For example, a rough surface can increase thermal emissivity by increasing the effective emitting surface area.

The potential of the third category is interesting for future development and study. In this article, we will explore the performance of a theoretically designed TBC that aims to have both high solar reflectance and high emissivity. To achieve this, we present experimental investigations that highlight the effect of these properties, along with numerical analysis to assess the potential benefits of deploying "HE-HR-TBC" materials at a city scale to improve outdoor thermal comfort and reduce the UHI effect.

2.2. TBC to Reduce UHI?

Urban areas absorb and retain more solar energy due to their darker color and higher heat capacity. However, to reduce urban surface temperatures and mitigate the effects of the Urban Heat Island, pavements with specific properties (such as TBCs) can release/reflect energy stored/received by the environment. Several authors have analyzed the performance of different solutions, particularly on the use of highly reflective and/or emissive surfaces.

Tsoka et al. [52] made a review on the ENVI-met microclimate model and the use of cool materials and urban vegetation to simulate UHIs [52]. They investigated, among other things, the application of "cool" materials on ground and building envelope surfaces and their combination with urban vegetation. Technologies cited in their works as "cool" materials can modify solar reflection and absorption, increase evaporation, and change the

heat storage of pavements. They cited high emissive TBCs but resumed only results about reflective TBCs applied on the building envelope.

The study by Brito Filho and Santos [46] presented results highlighting the effectiveness of different strategies that involve modifying the properties of various surfaces to reduce energy consumption and mitigate the effects of Urban Heat Islands. The study recommends using a roof with thermal insulation and a selective coating in cities with an equatorial climate. Conversely, applying white paint to a roof without thermal insulation is recommended in towns with a subtropical climate. The study refers to using a selective coating without specifying its nature. Still, it does indicate some of its properties, such as high emissivity and reflectance coefficients (0.9) and a thermal conductivity of 0.00345 W/m.K.

This observation is shared by Di Giuseppe et al. [53]. The author provides a numerical study on the impact of roof reflectivity and the thermal transmittance of the building envelope on the Urban Heat Island effect in urban contexts in Italy. The study aims to understand the correlation between the optical properties of building coatings and the thermal transmittance of the applied envelope, as well as their influence on UHIs. The results indicate that using reflective materials, specifically those falling into the HE-HR-TBC class, could reduce the outdoor air temperature by 1.5 to 2 °C, depending on the specific configuration of the building envelope and geographical location.

The article by Khare et al. [54] examines the effects of the Urban Heat Island caused by dark surfaces in urban areas that absorb solar heat and increase the surface temperature. It explores strategies to mitigate this effect, including using "cool" roofs with high solar reflectance and thermal emissivity. These roofs help maintain a surface temperature 25 to 35 °C lower than traditional roofs. In India, where the climate is tropical, and building construction is growing, adopting cool roofs could result in significant energy savings. The study's results show a 49% reduction of thermal flux, which translates to an overall 8.8% energy saving for cooling. However, the author emphasizes that an integrated systemic approach is recommended to improve building performance and reduce heat islands. The sole use of these technologies cannot achieve the best results. Additionally, the author mentions that the high cost of these coatings and maintenance challenges pose major obstacles to their widespread adoption.

The article by Yang et al. [55] compares, through numerical simulations, the effectiveness of cool roofs and green roofs in mitigating Urban Heat Islands (UHIs) in a tropical climate, such as Singapore. The study results show that during peak periods (from 9 a.m. to 5 p.m.), the cool roofs reduce the heat gain by approximately 0.14 kWh.m^{-2} (8%). It should be noted that the authors simulated theoretical coatings considered "cool" due to their thermal properties (emissivity and reflectance).

These findings appear to be theoretically promising, although the studies have not been conducted on commercially available products and lack concrete applications. It is important to note that reflected radiation can unintentionally be trapped or reflected onto adjacent buildings or pedestrians, leading to overheating and thermal discomfort [56]. A multimodal approach, utilizing the simultaneous implementation of different strategies, appears to be an optimized pathway for mitigating Urban Heat Islands.

In contrast to the existing literature, our numerical approach will be based on an existing coating previously tested in a controlled environment. We focused our numerical study on the variability of radiative properties of city faces (ground, roof, wall) and their placement to evaluate the impact on UHIs. The coupling of this approach with other aspects of the previously cited multimodal approach could be the subject of future work.

3. Materials and Methods

Our analysis is conducted using a two-fold methodology. The first part involves experimental testing of a nano-ceramic-based HE-HR-TBC at a local scale (building level) to evaluate its performance. Subsequently, we extended this methodology to a global scale (city-level) to assess the potential of the studied HE-HR-TBC in mitigating Urban Heat

Island effects, reflected in its impact on pedestrian outdoor thermal comfort. The entirety of the method employed in our work is summarized in Figure 1.

Figure 1. Methodology applied in this work.

3.1. Experimental Studies

We then present the model used in our experimental study, the measuring instruments, and the scenarios.

3.1.1. Experimental Design and Procedure

The experimental setup comprises a small-scale support structure with a removable roof. This structure is in an enclosed room equipped with a high-capacity air conditioning system, enabling us to adjust the ambient temperature. The activation of the air conditioning system is dependent on the experimental scenarios. The model's walls (walls and floor) have a total thickness of 38 mm, composed of 2 faces of plywood (1 with a thickness of 3 mm and the other with 15 mm) and a 20 mm layer of expanded polyurethane.

The small-scale support comprises five rooms 57 cm wide and 88 cm long (see Figure 2). The interior doors remain open during the experiment to ensure proper air circulation. To simulate solar radiation, we utilized 12 lamps arranged on a ramp, each with a power output of 300 W. These lamps were positioned 92 cm away from the roof. The lighting configuration was designed to achieve an approximate global irradiance of 1500 W.m^{-2}, assuming uniform illumination (see Figure 3). To simulate air ventilation, a fan is positioned at the center of one of the facades at a distance of 65 cm. The fan operates constantly, generating an airflow velocity exceeding 2 m.s^{-1}.

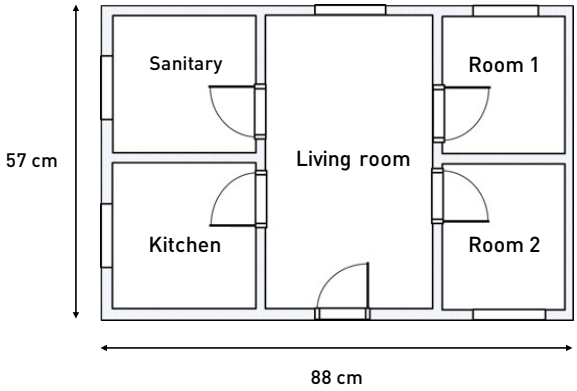

Figure 2. Model layout.

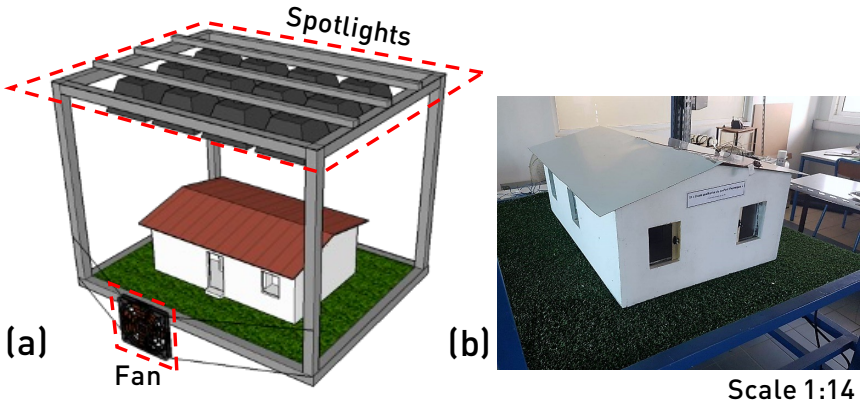

Figure 3. (**a**) Illustration of the small-scale test bench utilized for the experiments. (**b**) Picture of the small-scale (scale: 1:14).

Additionally, the experimental studies were conducted under two different overall thermal conditions: a controlled environment (room air-conditioning set at $T_{setpoint}$ = 26 °C) and an uncontrolled environment (no air-conditioning activated). The model's exterior windows and doors were adjusted accordingly, being fully open or closed based on the specific scenario requirements. Moreover, the lighting conditions were varied, with lights being partially illuminated (50%) or fully illuminated (100%).

3.1.2. Roofing Configurations and TBC Used

The experimental cell comprised five interchangeable steel sheet roofs in different colors (red, green, blue, gray, and white). Additionally, a sheet covered with a TBC was included. The TBC studied is a ceramic flake-based coating manufactured by Thermacote France. A high-pressure spray gun applies this TBC in two layers (0.5 mm/layer) on a white steel sheet roof. Between each coat, we observed a one-hour drying period. The manufacturer's specified properties are in Table 1, available at https://www.thermacote.fr/documentation/ (accessed on 21 June 2023). Unfortunately, no information is available on the size of the ceramic particles or the chemical composition of the solution. It can be classed as a HE-HR-TBC, and we will refer to it as such for the rest of this study.

Emissivity and reflectance are measurements of a material's thermal emission and light reflection capabilities, respectively. The specific emissivity values (in our case, 0.88) and reflectance (here, 0.83) depend on the material and can be influenced by surface roughness. The objective is often to balance between these two properties based on specific application requirements.

Table 1. Nano-ceramic-based HE-HR-TBC from "ThermaCote®" used in this study.

Appearance	Matte/rough
Color	hite
Density	0.41 g.cm^{-3}
Thermal conductivity	0.0345 W.m^{-1}.K^{-1}
Thermal emissivity	88%
Solar reflectance	83%

On Reunion Island, older homes are generally not insulated on the roof, whereas more recent or renovated buildings are more often insulated on the roof. To reflect this change, we chose to carry out measurements with and without insulation. The insulation used was rockwool in the form of a horizontal ceiling about 25 mm thick.

3.1.3. Measurement Techniques

A combination of data loggers and instruments was employed to capture the thermal behavior of the studied HE-HR-TBC. To ensure accurate readings, surface temperature measurements were obtained using type T thermocouples (copper/constantan) that were precalibrated under the same conditions. A surface heat flux meter was installed on the underside of the sheet to measure the thermal flux traversing the roof. Two synchronized data acquisition units, GRAPHTEC® and ALMEMO®, were used to record the temperatures of the lower roof surfaces and the heat flux passing through them.

Indoor and outdoor air temperatures were recorded using autonomous TESTO® data loggers, providing valuable information about the ambient air quality.

Due to the solar spectrum comprising a more significant proportion of infrared radiation (approximately 50%), most heat absorbed by urban surfaces is attributed to the near-infrared component [57]. This is how we utilized an Ocean Optics® spectrophotometer, model JAZ (see Figure 4), to compare the reflected electromagnetic spectrum profile of a roof covered in classic white paint to that of a roof equipped with a white Thermal Barrier Coating. We also compared the spectrum profile to that emitted directly by the spotlights. These measurements allowed us to understand and evaluate the reflected energy in the visible and near-infrared domains (from 200 to 1100 nm). The measure was conducted in two quasi-synchronous phases once the surface temperatures reached a steady state. Initially, the spectrophotometer cell was positioned orthogonally to one side of the roof at three different points. Subsequently, the cell was placed in the plane of three spotlights. The recording was instantaneous. The data from the various positions were then averaged.

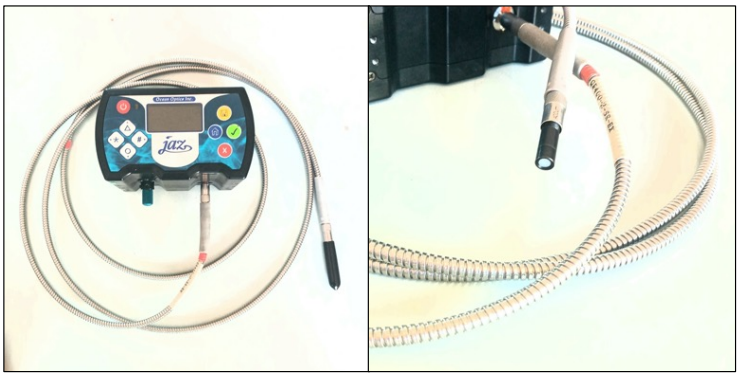

Figure 4. Ocean Optics® spectrophotometer, model JAZ, for spectrometric measurements.

3.1.4. Experimental Scenarios

All experimental scenarios were synthesized in Table 2.

Table 2. Experimental scenarios.

Scenario	Exterior Doors and Windows	Ambiant Air Conditioning	Spotlight		Ventilation		Ceiling with Thermal Insulation		Roof Coating					
			50%	100%	Without	With	Without	With	Red	Blue	Gray	Green	White	HE-HR-TBC
1			X		X		X		X	X	X	X	X	X
2				X	X		X		X	X	X	X	X	X
3	Open	ON		X		X	X		X	X	X	X	X	X
4				X	X			X	X	X	X	X	X	X
5				X		X		X	X	X	X	X	X	X
6	Open	OFF		X	X		X		X	X	X	X	X	X
7	Close	OFF		X	X		X		X	X	X	X	X	X

$T_{setpoint}$: 26 °C.

3.2. Numerical Studies

The objective of the numerical simulations is to assess the potential of the HE-HR-TBC on a more global scale in regulating building space temperatures and thereby reducing Urban Heat Islands (UHI). To achieve this, a digital protocol is implemented by comparing different scenarios of TBC usage, varying based on the surface area covered by the studied HE-HR-TBC.

3.2.1. Modeling Tool and Output Used

The simulations were conducted using Grasshopper in Rhino 6 with the Honeybee plugin. This powerful combination allowed for flexible parametric design and comprehensive analysis of the configurations. The simulations provided detailed insights into each configuration's thermal behavior and performance, highlighting the impact of the HE-HR-TBC on the studied environments.

To comprehensively investigate the influence of urban configurations on UHIs, our approach centers on the analysis of outdoor thermal perception utilizing the Universal Thermal Comfort Index (UTCI). The UTCI integrates parameters, such as air temperature, wind speed, humidity, and thermal radiation, to evaluate thermal sensations within an urban environment [58–60]. When implementing technical solutions, such as Thermal Barrier Coatings, to mitigate heat absorption by urban surfaces, the UTCI enables measurement of comfort changes before and after, thus assessing the potential attenuation of heat islands and enhancement of conditions for individuals while promoting an environment conducive to building energy efficiency; it is noteworthy that the accurate computation of the UTCI is ensured through the employed numerical simulation software. The Urban Thermal Comfort Index (UTCI), widely used in environmental studies to assess human thermal comfort in urban settings, similarly incorporates meteorological factors as UTCI does, providing a holistic measure of perceived thermal conditions, thus justifying our use of UTCI to examine the impact of Thermal Barrier Coatings on UTCI by the work of Wang et al. [61], given the close relationship between UTCI and ambient temperature.

3.2.2. Case Study

The numerical simulations were conducted within a geometric domain commonly employed in the literature [62–64]. The geometric domain described above can be visualized in Figure 5, which illustrates the layout and arrangement of the simplified city typology comprising the surface area of 123 m by 123 m and the nine identical buildings spaced at regular intervals. Each building within the domain measures 18 m by 18 m and has a height of 9 m. The buildings were uniformly spaced along the edges, maintaining a distance of 18 m between them, while the spacing between buildings remained consistent at 18 m throughout the domain. This simplified city typology served as a representative model to investigate the thermal behavior and performance of the studied configurations in a controlled and reproducible manner.

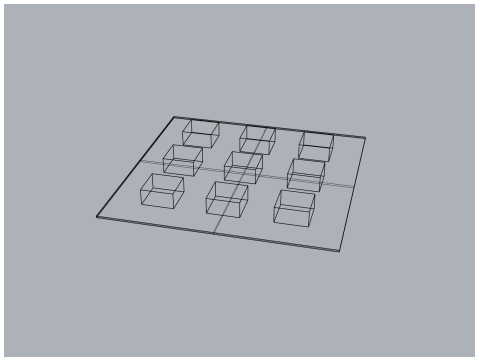

Figure 5. A perspective view of the geometrical model used in the simulation.

3.2.3. Climatic Conditions

The selected weather file (EPW files) for the simulations corresponds to the city of Le Port, located on Reunion Island. Le Port experiences a tropical climate with distinct wet and dry seasons. The annual climatic conditions of the city are characterized by high temperatures, averaging around 25 to 30 °C, throughout the year. The period selected for the simulations aligns with the summer period on Reunion Island, from November to March, between 6:00 a.m. and 6:00 p.m. These months exhibit intense solar radiation (varying between 1000 and 1200 $W.m^{-2}$), prolonged daylight hours, and elevated temperatures, making them crucial for assessing the studied configurations' thermal performance under the region's most challenging climatic conditions.

3.2.4. City Envelope Composition

The city envelope is composed of three different types of material. An "Asphalt Pavement" type material was used for the exterior floor. For the building envelope (roof and vertical walls), two types of material were used: 20 cm-thick concrete walls covered with a 1 mm-thick layer of the studied HE-HR-TBC, listed as "Wall N°2", and 20 cm-thick concrete walls covered on both sides with a 1 cm-thick layer of cement plaster, listed as "Wall N°1". The latter wall composition was chosen to represent a range of typical building constructions. All the physical properties of the materials are presented in Table 3.

Table 3. Physical properties of materials.

	Asphalt Pavement	**Wall N°1**	**Wall N°2**
Thickness (m)	0.2	0.01	0.201
Conductivity ($W.m^{-1}.K^{-1}$)	0.70	1.75	1.402
Specific heat ($J.kg^{-1}.K^{-1}$)	900	1000	1000
Thermal emissivity (-)	0.9	0.9	0.88
Solar reflectance (-)	0.3	0.5	0.83

3.2.5. Configurations Studied

We simulated seven configurations to evaluate the comparative effects of different material strategies on thermal quality and Urban Heat Island (UHI) mitigation. These configurations were created by combining various construction types, as described in Table 4.

The base case scenario (Configuration A) represents the absence of the HE-HR-TBC application, with vertical walls and roofs constructed using Wall N°1, and asphalt pavement on the ground. The remaining configurations (B, C, D, E, and F) involve the application of the studied TBC on different surfaces.

In Configuration B, the HE-HR-TBC is applied to the roof (Wall N°2), while the outdoor ground is asphalt pavement and the walls are constructed using Wall N°1 (concrete). Configuration C features the HE-HR-TBC applied to the outdoor ground (Wall N°2), with the roof and walls constructed using Wall N°1.

In Configuration D, the HE-HR-TBC is applied to the roof and outdoor ground (Wall N°2), while the walls are made of concrete (Wall N°1). Configuration E involves the HE-HR-TBC applied to the walls and outdoor ground (Wall N°2), with the roof constructed using Wall N°1 (concrete).

Lastly, Configuration F entails the application of the HE-HR-TBC on the walls, roofs, and outdoor ground, all constructed using Wall N°2.

Through this study, we aim to conclude the direct impact of applying this type of coating on UHI mitigation.

Table 4. Configuration of proposed scenarios.

Configuration	Description of the Configuration
A	Base case (no TBC)
B	HE-HR-TBC on roof, outdoor ground in asphalt pavement, and walls in concrete
C	HE-HR-TBC on outdoor ground, roof and walls in concrete
D	HE-HR-TBC on roof and walls, outdoor ground in asphalt pavement
E	HE-HR-TBC on walls and outdoor ground, roof in concrete
F	HE-HR-TBC on walls, roofs, and outdoor ground

4. Results and Discussions

4.1. Experimental Analysis on the HE-HR-TBC

In this first section, we conducted an experimental analysis on a test bench in a controlled climatic environment to confirm the performance of the TBC used and, most importantly, to verify its classification as a HE-HR-TBC material (high emissivity and high reflectance). Several results are presented based on the previously mentioned scenario table (see Table 2).

4.1.1. Surface Temperature Analysis—Scenario N°1 to N°5

The ambient temperature within the zone where the scaled-down prototype is situated is consistently maintained at 26 °C. In a general sense, as it can be seen in Table 5, there is an observed inclination for the blue-colored coating to manifest higher surface temperatures in the majority of scenarios, while the studied HE-HR-TBC is the most effective one to reduce roof surface temperatures in all scenarios, even compared to the white coating. This is in agreement with previous works [33–35,45].

Among the obtained results, a pertinent analysis pertains to comparing coupling strategies of solutions aimed at reducing surface temperatures. In particular, the comparison between Scenarios 3 and 5 enables us to study the impact of incorporating thermal insulation in the case of a test cell subjected to enhanced ventilation. In this context, we observe that the results for the HE-HR-TBC coating do not exhibit a significant difference (45.5 °C and 44.9 °C, respectively), even when considering a measurement error on the order of a degree Celsius. Also, in comparison to a white reflective coating, the HE-HR-TBC enhances roof temperature reduction by 27.3 °C and 19.1 °C, respectively, for Scenarios 3 and 5, as observed in [34].

Conversely, this observation does not apply to the other coating colors; quite the contrary: the presence of insulated attics leads to a noteworthy increase in the surface temperatures of the roofs. This escalation can likely be explained by the fact that the roof has a limited capacity for heat transfer through the thermal conduction toward the interior areas of the prototype due to the pronounced warming of the air zone situated beneath the roof (analogous to insulated attics), as well as the uninterrupted incidence of radiation on the roof originating from the projectors. With its high volumetric heat capacity, the steel persists in accumulating heat, notwithstanding the convective phenomena supported by ventilation. In contrast, the HE-HR-TBC coating tends to maintain a stable surface temperature, thus affirming two previously demonstrated properties: a high emissivity (the TBC-coated sheet scarcely, if at all, accumulates heat, as it re-emits it through radiation

toward the environment, which is cooler) and a high reflectivity, allowing for the redirection of the majority of the radiation received from the projectors.

Lastly, regarding Scenarios 4 and 5, which involve insulated attics, a comparison is established based on the presence or absence of mechanical ventilation. In contrast to prior observations, the results highlight the notable impact of convective phenomena induced by mechanical ventilation, with a temperature difference of approximately 5 °C in favor of the ventilation-integrated scenario for the TBC-coated sheet, similarly as in [44]. These findings are more nuanced for the blue and more pronounced for the white-colored sheet.

Table 5. Surface temperature reached for different scenarios.

Scenario	Roof Coating	$T_{roofsurface}$ [°C]
1	Red	67.6
	Blue	76.3
	Green	72.0
	White	62.4
	Gray	65.7
	HE-HR-TBC	55.8
2	Red	85.0
	Blue	96.3
	Green	88.1
	White	72.2
	Gray	102.4
	HE-HR-TBC	68.9
3	Red	85.6
	Blue	92.6
	Green	79.7
	White	64.6
	Gray	62.4
	HE-HR-TBC	45.5
4	Red	94.1
	Blue	99.0
	Green	84.2
	White	82.0
	Gray	86.4
	HE-HR-TBC	50.1
5	Red	93.6
	Blue	97.3
	Green	78.9
	White	72.2
	Gray	70.9
	HE-HR-TBC	44.9

The variations in roof surface temperatures among the different colors (red, blue, green, gray) appear to be correlated with their inherent properties. In building design, especially when considering thermal regulation requirements [65], colors often signify specific thermal absorptivity, reflectivity, and emissivity characteristics. Typically, darker colors have higher absorption coefficients, while lighter colors exhibit greater reflectivity. However, the results presented in Table 5 indicate the existence of additional factors that must be considered to describe the physical properties of coatings comprehensively. For instance, the gray coating closely resembles the white coating in specific scenarios.

These findings underscore the necessity for a standardized approach to precisely characterize the radiative properties of building wall surfaces, especially when aiming to achieve the effects of Thermal Barrier Coatings.

4.1.2. Comparative Analysis of Transmitted Heat Flux—Scenario N°6

In this analysis, the ambient temperature of the room where the experiment occurs is not controlled. The interior doors are left open, and the exterior openings are closed. The ventilation is not activated (Scenario N°6, in Table 2).

The fluxmeter is attached to the underside of the roof, in the same position for each sheet. This experimental setup allows us to compare the amount of thermal flux transmitted inside the model. This helps us evaluate the conductive contribution to the insulating capacity of the roof coated with the HE-HR-TBC. This configuration is similar to what is typically found in real-life situations, where most heat gains occur through the roof, particularly in hot environments.

Therefore, we compared the roof colors to the one equipped with the HE-HR-TBC (see Figure 6). The results are as follows: the transmitted flux through the nano-ceramic based-TBC-coated sheet is the lowest (around 50 W.m^{-2} under steady-state conditions), which is very close to the flux transmitted by the white sheet (55 W.m^{-2}). The gray roof is the least efficient, with a transmitted flux of over 165 W.m^{-2}.

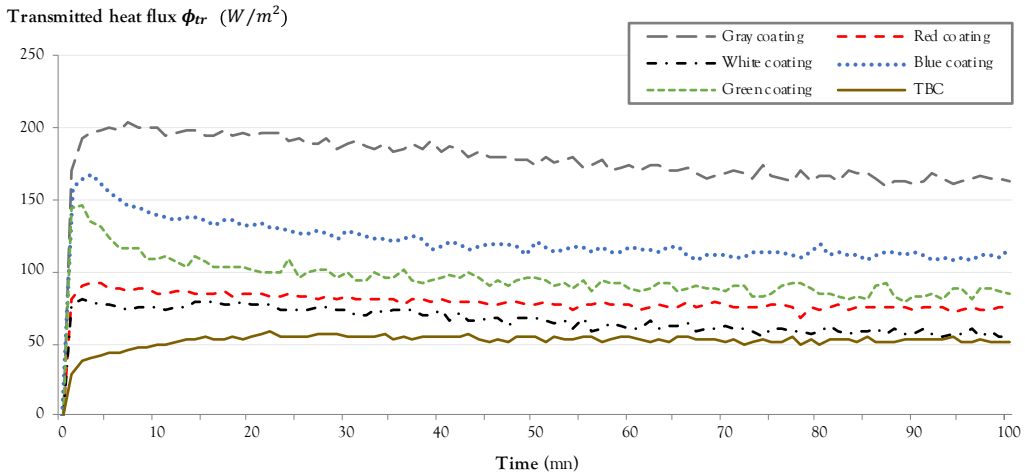

Figure 6. Comparison of the heat flux transmitted for various roof colors and for the roof equipped with the HE-HR-TBC (no ventilation, no imposed ambient temperature).

The following ratios can be used to assess the potential of the HE-HR-TBC: the TBC-equipped roof reduces the transmitted energy by 70% compared to a gray roof but remains close to the regular white roof with a decrease of approximately 10% under steady-state conditions.

In this context, we observed that the white HE-HR-TBC-coated roof appears to limit conductive transfers, which can be further confirmed through subsequent experiments. However, it is important to note that this technology does not significantly contribute to conductive heat transfers (which is logical given the thickness of the coating).

4.1.3. Comparative Spectral Reflectance Analysis—Scenario N°6

In this new study, the configurations remained the same as in the previous analysis (Scenario N°6, as shown in Table 2). In this specific scenario, and taking into account the conclusions drawn from the flux measurements (refer to the previous section), spectral analyses were exclusively conducted on both the uncoated white sheet and the one coated with the investigated HE-HR-TBC.

The measurements conducted using a spectroradiometer allowed the evaluation of the amount of energy re-emitted by two types of roofs: a conventional white roof and a roof coated with a white TBC coating (see Figure 7). The spectrum of the light spots was also overlaid to assess the proportion of energy emitted at different wavelengths.

We observed that both roofs exhibited similar behavior in the visible domain, indicating similarity in their response to light illumination despite the TBC coating and its matte surface. In the wavelength range of 380 to 780 nm, the roof with the TBC coating

reflected a cumulative sum of 91.2 W.m^{-2}, while the white roof reflected 93.6 W.m^{-2}. The difference becomes more pronounced in the near-infrared (between 780 nm and 1040 nm, "IR-A"), where the spectral irradiance is higher for the roof with the TBC coating, with a cumulative difference of 13 W.m^{-2}. This observation signifies a higher reflectivity of the TBC-coated roof in this spectral range. It is important to note that the reflective behavior of the TBC coating varies with the spectral domain. Although it has minimal impact in the visible range, its reflectivity is higher in the infrared. This characteristic highlights the strong potential for the infrared retro-reflection of the TBC coating.

The significant variability in spectral irradiance, particularly in the nearby bands starting from 930 nm, can also be attributed to the surface condition of the studied roofs: the matte surface of the TBC coating appears to reduce the impact of reflected radiation, unlike the smooth surface of the white roof.

These results warrant further investigation across broader spectral ranges to confirm these trends and explore the potential of the TBC coating in the mid-infrared (IR-B), which corresponds to wavelengths above 1040 nm. A more detailed analysis would provide a better understanding of the mechanisms involved in the TBC coating's reflection and re-emission of thermal energy across different portions of the infrared spectrum.

The observed behavior of the TBC coating, characterized by higher reflectivity in the near-infrared range (IR-A) and infrared retro-reflection, can be interpreted as an indication of a high emissivity of the TBC coating.

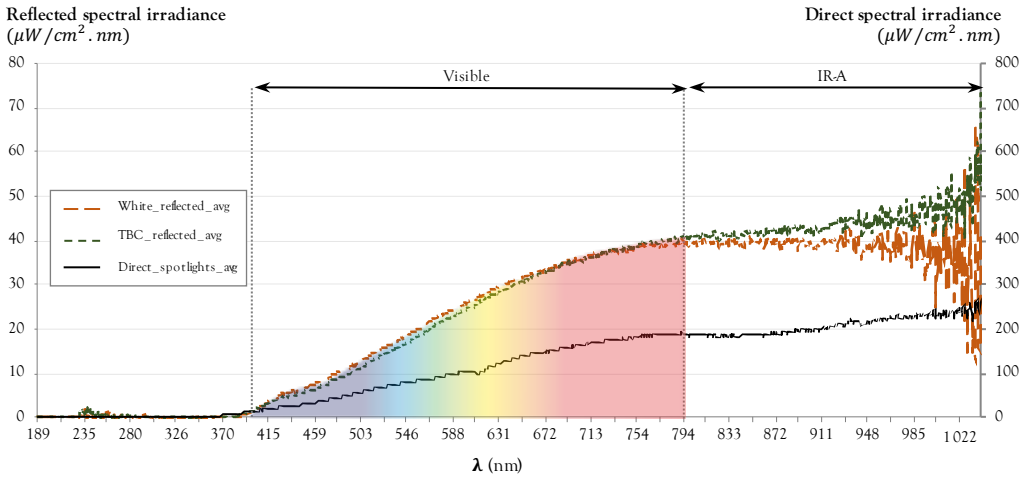

Figure 7. Comparison of the amount of reflected energy per wavelength for TBC and white coating, as a function of the amount of direct energy coming from the spotlights.

4.1.4. Indoor and Outdoor Ratio and Linearized Slope Analysis—Scenario N°7

In Scenario N°7, we chose to investigate the impact of the roof on indoor environmental conditions under unfavorable circumstances. We considered a case where the facade openings are closed, the air conditioning is turned off, and the mechanical ventilation is deactivated. This scenario represents a fully enclosed house in a climatic context characterized by clear skies and the absence of external wind. Our study evaluates indoor air temperatures by comparing the color variations of a roof with and without the HE-HR-TBC.

The experiments were conducted on the same model at different times to avoid any influence from one configuration to another due to residual heat. Since the overall ambient temperatures were not controlled, a gap inevitably exists between the initial indoor and outdoor air temperatures. All the experiments thus enabled us to measure the temperature variations over 100 min, all synchronized by the activation of the light spots.

We chose to present the ratio between the indoor and outdoor temperatures, as well as the linearized slope (passing through the origin) of the linear trend curves for each result (see Figures 8 and 9). These pieces of information allow us to interpret the thermal inertia of the model, with only variations in the roof color and the presence of the HE-HR-TBC.

We observed that the temperature ratio's evolution for all the colored roofs follows a similar trend: an initial plateau for the first 10 min, followed by an exponential increase until reaching what could be considered another plateau after 90 min of the experiment. The temperature ratio curve for the TBC exhibits a distinctly different pattern, ultimately showing minimal variation between the beginning and end of the experiment. This behavior once again demonstrates the emissive power of the HE-HR-TBC-coated roof. When an emissive material absorbs thermal energy, it can efficiently re-emit it, which contributes to dissipating heat and maintaining a more stable temperature. In our case, the constancy of the ratio reflects this behavior of the TBC, reaching a steady-state ratio very close to that of the white roof.

These findings are supported by the study of the linear trend curve's evolution (linearized slope passing through the origin) for each indoor air temperature within the model, as illustrated in Figure 9. This information reflects the thermal inertia of the experimental setup. We observed that the mere presence of the TBC coating significantly reduces the amplitude of the temperature variations indoors.

The linearized slope for the TBC coating is 0.0606, compared to 0.1093 for the white roof and 0.1556 for the gray roof. This means it takes approximately 39% more time for the model with the TBC coating to increase its temperature by a similar magnitude compared to the model with the gray roof.

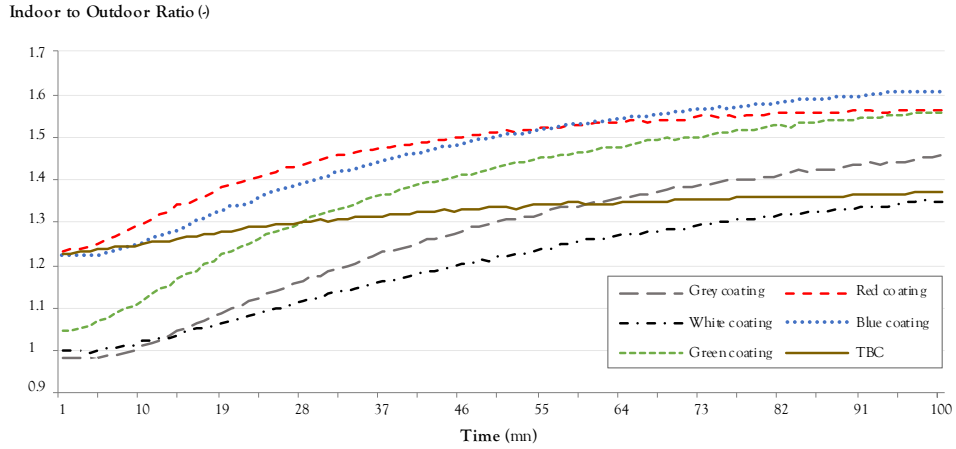

Figure 8. Indoor and outdoor air temperature ratio.

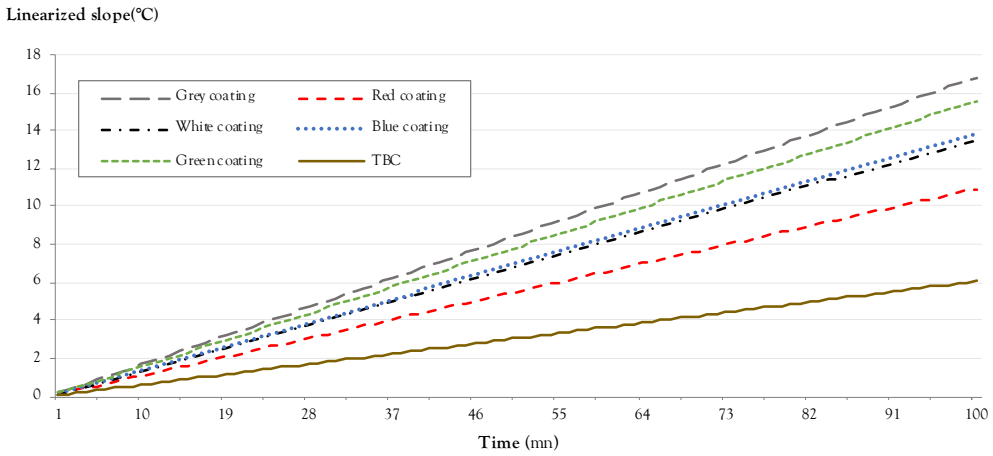

Figure 9. Linearized slope analysis (thermal inertia indicator).

This indicates a significant reduction in energy transmission, confirming the previous results. Given that the TBC's insulating capacity in terms of heat transfer by conduction

is limited to its thickness, we deduced that its predominant action occurs in radiative transfers, which are regulated by its emissivity and reflectance properties.

Given all of these results, we now aim to assess the potential of this technology in reducing Urban Heat Islands. A numerical approach was chosen to achieve this, and the results are described below.

4.2. Numerical Analysis: HE-HR-TBC to Reduce UHI?

In this section, we propose to study the values of a widely used indicator for calculating outdoor comfort, the UTCI. As the UTCI strongly correlates with air temperature [61], we use it here to discuss the TBC's effect on UHIs. This indicator is calculated on a plane composed of a mesh of 2 m × 2 m cells. To check the impact of the height of the position of this calculation plane, we calculated the UTCI for three z values (z = 1 m, z = 2 m, and z = 4 m). Z is the height of the UTCI calculation plane. These heights correspond to the pedestrian level, commonly referenced in the literature.

The results in Figure 10, which showcase the UTCI heatmap for Configuration A and Configuration F, provide an insightful analysis. These two configurations represent the most contrasting scenarios in terms of the composition of the building envelope. Surprisingly, this figure reveals a nearly identical spatial distribution pattern of the UTCI for both configurations. This indicates that the spatial distribution of the UTCI is minimally influenced by the addition of a Thermal Barrier Coating (TBC) within the studied domain. However, the notable difference lies in the temperature ranges presented in the heatmap. The addition of the TBC significantly impacts the specific temperature ranges experienced within the domain. This suggests that while the overall spatial distribution remains relatively unchanged, the TBC influences the localized thermal conditions, resulting in distinct temperature variations across the building envelope.

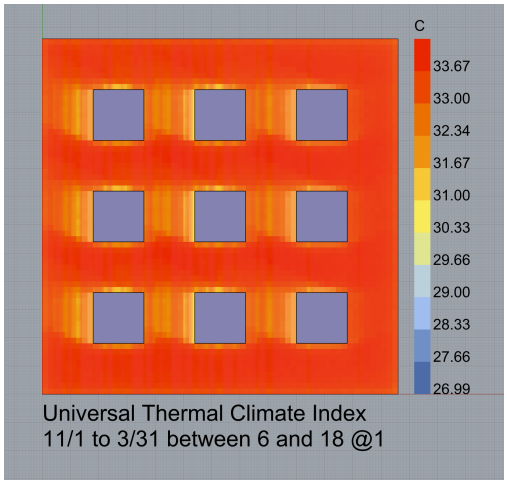

UTCI map for Configuration A at z = 2 m

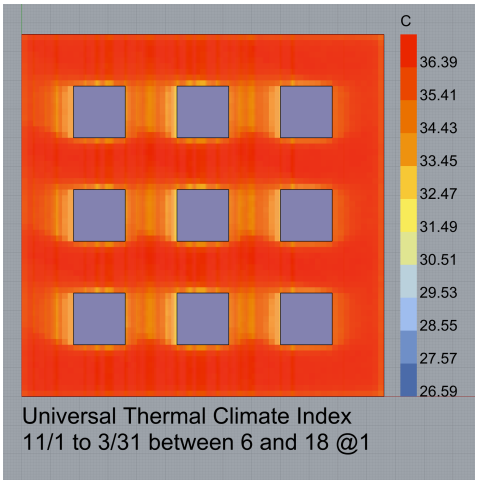

UTCI map for Configuration F at z = 2 m

Figure 10. UTCI map for Configurations A and F.

In Table 6, the thermal performance of different configurations with the HE-HR-TBC application was analyzed using the UTCI at varying heights of calculation (z). The UTCI mean values exhibited consistent results across all configurations, ranging between approximately 31.53 and 33.58, indicating a moderate thermal comfort level. However, the UTCI max values showed slight variations, with configurations B, C, D, E, and F consistently displaying higher values than the base case (Configuration A). Notably, Configuration D demonstrated the highest UTCI max values across all heights of calculation.

Table 6. UTCI results for simulated scenarios on a plane at three different z heights (in °C).

	Height of UTCI Calculation z = 1 m		Height of UTCI Calculation z = 2 m		Height of UTCI Calculation z = 4 m	
Configuration	**UTCI Mean Value**	**UTCI Max Value**	**UTCI Mean Value**	**UTCI Max Value**	**UTCI Mean Value**	**UTCI Max Value**
A	31.73	33.76	31.71	33.65	31.53	33.40
B	31.74	33.74	31.71	33.69	31.53	33.42
C	33.45	36.46	33.58	36.44	33.44	33.22
D	31.73	33.75	31.71	33.65	31.56	33.42
E	33.45	36.46	33.58	36.42	33.45	36.19
F	33.44	36.47	33.58	36.45	33.44	36.20

Interestingly, the calculation height (z) did not significantly influence the UTCI values within the 1 m, 2 m, and 4 m range. These findings contribute to our understanding of the thermal performance of different configurations with a TBC and provide insights into potential discomfort or thermal stress levels in built environments. Adding an HE-HR-TBC to building surfaces can impact the UTCI, which assesses thermal comfort levels. We observed several trends by analyzing the results from different configurations with the TBC application. Based on the table comparing Configuration A with other configurations, it can be concluded that the reflective properties of the HE-HR-TBC lead to an increase in UTCI values, regardless of the height of calculation (z).

This implies that applying a TBC leads to an elevation in the outdoor felt temperature, as illustrated by the elevated UTCI values observed in configurations B, C, D, E, and F compared to the baseline scenario (Configuration A). The observed upswing in the UTCI indicates an escalation in thermal stress encountered by individuals within the urban environment. Integrating highly reflective materials on walls and floors contributes to amplifying radiative interactions between buildings and their environment. These aspects have been previously documented by Erell et al. [66], who examined the consequences of employing high-albedo materials on the thermal comfort of pedestrians using computational models. Their findings unveiled that even though the surrounding air temperature might decrease, this reduction proves insufficient in counterbalancing the augmented radiation loads. Consequently, the thermal comfort of pedestrians might be compromised.

In a study conducted in Egypt, characterized by a hot and arid climate, Faragallah and Ragheb [67] employed ENVI-MET to investigate the comfort of pedestrians near a street with vehicular traffic. They explored various scenarios involving the implementation of cool pavements. The simulation results demonstrated that the proposed layout led to a lesser degree of outdoor thermal comfort when compared to the existing conditions. Thus, implementing TBCs could result in a deterioration of thermal comfort conditions. Our findings align with the current body of literature, showcasing a similar trend.

The UTCI mean values exhibited a relatively consistent pattern across all the configurations, signifying that the inclusion of a TBC had a limited impact on the overall average thermal comfort level. However, more pronounced discrepancies were evident in the UTCI max values, representing peak thermal stress. The configurations incorporating the HE-HR-TBC application consistently demonstrated higher UTCI max values when compared to the baseline scenario without a TBC (Configuration A). This observation implies that a TBC could potentially result in localized zones of heightened thermal stress, which could lead to discomfort for occupants. Interestingly, Configuration D consistently showcased the highest UTCI max values among all the configurations. This suggests that the interplay of a TBC on the roof and outdoor ground, coupled with walls made of concrete, yielded the most substantial impact on the thermal stress of pedestrian levels. This finding underscores the critical nature of meticulously considering specific configuration elements when evaluating TBCs' efficacy in mitigating thermal stress. Notably, the variation in calculation height (z) exerted minimal influence on the UTCI values across the examined range of 1 m, 2 m, and 4 m. This implies that the vertical placement of the calculation point does not significantly alter the thermal comfort levels, regardless of whether a TBC is present. The introduction of a TBC across diverse configurations influenced the UTCI max values, thereby hinting at potential disparities in localized thermal stress levels. While the

UTCI mean values remained relatively stable, it remains crucial to meticulously account for specific configuration elements to optimize the TBC advantages and ensure occupant comfort in built environments.

Our observations indicate that applying a High-Emissive and High-Reflective Thermal Barrier Coating (HE-HR-TBC) in various locations across a city yields marginal effects on the overall ambient air temperature within the constructed environment. This leads us to the conclusion that the efficacy of a coating at a localized level might not readily extrapolate to its effectiveness on a broader, city-wide scale. Consequently, it becomes imperative to integrate a spectrum of technologies, including green spaces, water features, urban morphology, and the like, to realize the comprehensive and efficient mitigation of Urban Heat Island effects at the global level.

It is crucial to emphasize that the conclusions drawn from our numerical simulations are contingent upon the distribution of the UTCI comfort index. Had we focused on surface temperatures in various urban areas, we might have obtained divergent observations regarding this index, with conclusions akin to those derived from our experimental analyses; notably, that the HE-HR-TBC significantly reduces surface temperatures in urban environments. In our case, the deliberate choice of the UTCI as a metric stems from the intention to achieve the most accurate possible representation of the impact of Urban Heat Islands on individuals, like in several other studies [54,68,69].

5. Conclusions and Perspectives

In light of these comprehensive analyses, we can now provide a preliminary response to the fundamental question that guided this study: Can nano-ceramic-based Thermal Barrier Coatings simultaneously enhance the energy efficiency of buildings and contribute to mitigating the effects of Urban Heat Islands at the city scale?

Indeed, our investigations have unveiled several significant elements:

- A thorough analysis of the state of the art reveals a lack of established consensus regarding the terminology associated with Thermal Barrier Coatings (TBCs), necessitating clarification.
- In response to this gap, we have proposed a classification into three categories: highly reflective and low emissivity coatings, referred to as "HR-LE-TBCs"; highly emissive and low reflectivity coatings coupled with insulation, termed "HE-LR-TBCs"; and, finally, the combination of both radiative properties, designated as "HE-HR-TBCs".
- Among these typologies, the "HR-LE-TBC" has undergone the most extensive investigation within the literature despite being designated as the least efficient for the targeted applications.
- The existing scientific literature does not adequately address the central issue of our research, as studies either focus on local or global scales. A cross-analysis of TBC performance across different scales is lacking.
- Our local-scale experiments (building level) demonstrate the indisputable effectiveness of nano-ceramic-based TBCs. They result in significant reductions in surface temperatures, improvements in indoor ambient conditions, a notable decrease in heat transfer through the roof, and the substantial reflection of near-infrared radiation.
- Our numerical simulations, on the other hand, have revealed a nuanced range of outcomes concerning the performance of the same TBC, evaluated under different urban configurations involving variations in the percentage of surfaces coated with the TBC. While our experimental studies suggested a potential reduction in surface temperatures at the building level, the coating itself, characterized by its high emissivity and pronounced reflectivity, would tend to elevate the outdoor heat stress level. This trend would lead to discomfort outdoors, positioning buildings and individuals within hot thermal islands, thereby creating an environment unfavorable to their overall efficiency and well-being.

After our investigation, in response to our research question, a definitive conclusion arises in the specific context of our study: Nano-ceramic-based TBCs, despite their tangible

benefits for the efficiency of built structures, cannot be regarded as a directly transferable and generalizable solution outdoors to counter the adverse effects of Urban Heat Islands and to enhance comfort within urban environments. This is partly due to the risk of the overuse of TBCs, which could result in excessively emissive and reflective urban surfaces, potentially inducing outdoor thermal discomfort.

For more comprehensive analyses, and within the scope of future work, we will quantify the direct impact of TBCs on buildings while exploring their indirect influence on Urban Heat Islands by reducing anthropogenic heat inputs (notably air conditioning emissions). We will also seek to evaluate the potential of an integrated urban approach, combining various solutions (coatings, water bodies, vegetation, urban layout) and its impact on the overall efficiency of structures.

Finally, to better comprehend the thermal behavior of the studied HE-HR-TBC, we will seek to chemically characterize it and observe any changes in the size and quantity of ceramic particles before and after the spraying process.

Author Contributions: B.M.-D.: investigation, data curation, writing—original draft, visualization, methodology, validation, writing—review and editing; D.B.: conceptualization, methodology, writing—review and editing, validation; G.R.: conceptualization, methodology, investigation, data curation, writing—review and editing, validation. All authors have read and agreed to the published version of the manuscript.

Funding: This research received no external funding.

Institutional Review Board Statement: Not applicable.

Informed Consent Statement: Not applicable.

Data Availability Statement: Data is unavailable.

Acknowledgments: We thank the PIMENT laboratory technician, Jérôme VIGNERON, and SOVELO for making this product available.

Conflicts of Interest: The authors declare no conflicts of interest.

References

1. Nahar, N.M.; Sharma, P.; Purohit, M.M. Performance of different passive techniques for cooling of buildings in arid regions. *Build. Environ.* **2003**, *38*, 109–116. [CrossRef]
2. Rahimi, J.; Poursaeidi, E.; Montakhabi, F.; Sigaroodi, M.R.J.; Jamalabad, Y.Y. Experimental and numerical life evaluation of TBCs with different BC and diffusion coating under cyclic thermal loading. *Int. J. Appl. Ceram. Technol.* **2023**, *20*, 2888–2918.
3. Zhan, H.; Ma, W.; Han, X.; Liang, W.; Hao, J.; Dong, H.; Bai, Y.; Liu, H.; Meng, X. A new type of Sr(Zr0.2Hf0.2Ce0.2Yb0.2Me0.2)O3-x (Me = Y,Gd) high-entropy ceramics used in thermal barrier coatings. *Int. J. Appl. Ceram. Technol.* **2023**, *20*, 1764–1773.
4. Ericks, A.R.; Zok, F.W.; Poerschke, D.L.; Levi, C.G. Protocol for selecting exemplary silicate deposit compositions for evaluating thermal and environmental barrier coatings. *J. Am. Ceram. Soc.* **2022**, *105*, 3665–3688.
5. Hossain, M.K.; Rubel, M.; Akbar, M.A.; Ahmed, M.H.; Haque, N.; Rahman, M.F.; Hossain, J.; Hossain, K.M. A review on recent applications and future prospects of rare earth oxides in corrosion and thermal barrier coatings, catalysts, tribological, and environmental sectors. *Ceram. Int.* **2022**, *48*, 32588–32612. [CrossRef]
6. Lashmi, P.G.; Aruna, S.T. An Overview of Plasma-Sprayed Thermal Barrier Coating Activities in India. In *A Treatise on Corrosion Science, Engineering and Technology*; Kamachi Mudali, U., Subba Rao, T., Ningshen, S., G. Pillai, R., P. George, R., Sridhar, T.M., Eds.; Springer: Singapore, 2022; pp. 733–753. [CrossRef]
7. Thakare, J.G.; Pandey, C.; Mahapatra, M.M.; Mulik, R.S. Thermal Barrier Coatings—A State of the Art Review. *Met. Mater. Int.* **2021**, *27*, 1947–1968. [CrossRef]
8. Liang, L.; Wei, H.; Chang, X.; Xu, W.; Li, X.; Wei, Y. Enhanced insulation temperature and the reduced thermal conductivity of nanostructured ceramic coating systems. *Int. J. Heat Mass Transf.* **2013**, *65*, 219–224. [CrossRef]
9. Satyavathi Yedida, V.; Vasudev, H. A review on the development of thermal barrier coatings by using thermal spray techniques. *Mater. Today Proc.* **2022**, *50*, 1458–1464.
10. Ghosh, S. Thermal properties of glass-ceramic bonded thermal barrier coating system. *Trans. Nonferrous Met. Soc. China* **2015**, *25*, 457–464. [CrossRef]
11. Liu, L.; Wang, S.; Zhang, B.; Jiang, G.; Liu, H.; Yang, J.; Wang, J.; Liu, W. Present status and prospects of nanostructured thermal barrier coatings and their performance improvement strategies: A review. *J. Manuf. Process.* **2023**, *97*, 12–34. [CrossRef]

12. Reghu, V.; Mathew, N.; Tilleti, P.; Shankar, V.; Ramaswamy, P. Thermal Barrier Coating Development on Automobile Piston Material (Al-Si alloy), Numerical Analysis and Validation. *Mater. Today Proc.* **2020**, *22*, 1274–1284.
13. Kiełczawa, T.; Sokolowski, P.; Małachowska, A. The Influence of the Substrate Topography on the Plasma Jet Flow and Particle Deposition as a Determining Factor of Thermal Barrier Coatings Build-Up Mechanisms in Plasma Spraying. In Proceedings of the ITSC2021, Quebec City, QC, Canada, 24–28 May 2021.
14. Wei, Z.Y.; Meng, G.H.; Chen, L.; Li, G.R.; Liu, M.J.; Zhang, W.X.; Zhao, L.N.; Zhang, Q.; Zhang, X.D.; Wan, C.L.; et al. Progress in ceramic materials and structure design toward advanced thermal barrier coatings. *J. Adv. Ceram.* **2022**, *11*, 985–1068. [CrossRef]
15. Kumar, A.; Moledina, J.; Liu, Y.; Chen, K.; Patnaik, P.C. Nano-Micro-Structured 6 Comprehensive Review of Comparative Performance Analysis. *Coatings* **2021**, *11*, 1474. [CrossRef]
16. Wu, Y.; He, D. NdYbZr2O7 thermal barrier coating resistant to degradation by volcanic ash and CMAS. *Corros. Sci.* **2022**, *209*, 110795. [CrossRef]
17. Huang, J.; Chu, X.; Yang, T.; Fang, H.; Ye, D.; Wang, W.; Zhang, X.; Sun, W.; Huang, R.; Li, C.J. Achieving high anti-sintering performance of plasma-sprayed YSZ thermal barrier coatings through pore structure design. *Surf. Coatings Technol.* **2022**, *435*, 128259. [CrossRef]
18. Wang, S.; Liu, X.; Zhang, Z.; Zhu, J.; Li, Z. Research Progress on Thermal Barrier Insulation Coatings. *Highlights Sci. Eng. Technol.* **2022**, *20*, 173–185. [CrossRef]
19. Luo, L.; Chen, Y.; Zhao, X. 11—Strategies for improving the lifetime of air plasma sprayed thermal barrier coatings. In *Thermal Barrier Coatings*, 2nd ed.; Guo, H., Ed.; Woodhead Publishing Series in Metals and Surface Engineering; Woodhead Publishing: Cambridge, UK, 2023; pp. 325–360. [CrossRef]
20. Song, J.; Sun, B.; Xing, Y. Thermo-structural behavior of thermal barrier coatings for thrust chamber applications. *Int. Commun. Heat Mass Transf.* **2022**, *130*, 105776. [CrossRef]
21. Bogatyrev, A.; Liao, Z.; Axinte, D.; Norton, A. Tailorable shielded compliance of thermal barrier coatings through laser texturing and microstructural modification: Microfeature design and validation. *J. Eur. Ceram. Soc.* **2023**, *43*, 3704–3726. [CrossRef]
22. Barwinska, I.; Kopec, M.; Kukla, D.; Senderowski, C.; Kowalewski, Z.L. Thermal Barrier Coatings for High-Temperature Performance of Nickel-Based Superalloys: A Synthetic Review. *Coatings* **2023**, *13*, 769. [CrossRef]
23. Uchida, N. A review of thermal barrier coatings for improvement in thermal efficiency of both gasoline and diesel reciprocating engines. *Int. J. Engine Res.* **2022**, *23*, 3–19.
24. Zhou, X.; Song, W.; Yuan, J.; Gong, Q.; Zhang, H.; Cao, X.; Dingwell, D.B. Thermophysical properties and cyclic lifetime of plasma sprayed SrAl12O19 for thermal barrier coating applications. *J. Am. Ceram. Soc.* **2020**, *103*, 5599–5611.
25. Vaßen, R.; Jarligo, M.O.; Steinke, T.; Mack, D.E.; Stöver, D. Overview on advanced thermal barrier coatings. *Surf. Coatings Technol.* **2010**, *205*, 938–942.
26. Lee, S.W.; Lim, C.H.; Salleh, E.I.B. Reflective thermal insulation systems in building: A review on radiant barrier and reflective insulation. *Renew. Sustain. Energy Rev.* **2016**, *65*, 643–661. [CrossRef]
27. De Luca, P.; Carbone, I.; Nagy, J.B. Green building materials: A review of state of the art studies of innovative materials. *J. Green Build.* **2017**, *12*, 141–161.
28. Pisello, A.L. State of the art on the development of cool coatings for buildings and cities. *Sol. Energy* **2017**, *144*, 660–680. [CrossRef]
29. Rawat, M.; Singh, R. A study on the comparative review of cool roof thermal performance in various regions. *Energy Built Environ.* **2022**, *3*, 327–347. [CrossRef]
30. Modest, M. *Radiative Heat Transfer*; Academic Press: Cambridge, MA, USA, 2013. [CrossRef]
31. Bozsaky, D. Laboratory Tests with Liquid Nano-ceramic Thermal Insulation Coating. *Procedia Eng.* **2015**, *123*, 68–75. [CrossRef]
32. Bozsaky, D. Application of Nanotechnology-Based Thermal Insulation Materials in Building Construction. *Slovak J. Civ. Eng.* **2016**, *24*, 17–23. [CrossRef]
33. Uemoto, K.L.; Sato, N.M.; John, V.M. Estimating thermal performance of cool colored paints. *Energy Build.* **2010**, *42*, 17–22.
34. Dornelles, K.; Roriz, M.; Roriz, V.; Caram, R. Thermal performance of white solar-reflective paints for cool roofs and the influence on the thermal comfort and building energy use in hot climates. In Proceedings of the ISES Solar World Congress 2011, Kassel, Germany, 28 August–2 September 2011. [CrossRef]
35. Shen, H.; Tan, H.; Tzempelikos, A. The effect of reflective coatings on building surface temperatures, indoor environment and energy consumption—An experimental study. *Energy Build.* **2011**, *43*, 573–580. [CrossRef]
36. Kültür, S.; Türkeri, N. Assessment of long term solar reflectance performance of roof coverings measured in laboratory and in field. *Build. Environ.* **2012**, *48*, 164–172. [CrossRef]
37. Walker, R.; Pavía, S. Thermal performance of a selection of insulation materials suitable for historic buildings. *Build. Environ.* **2015**, *94*, 155–165. [CrossRef]
38. Azemati, A.A.; Shirkavand Hadavand, B.; Hosseini, H.; Salemi Tajarrod, A. Thermal modeling of mineral insulator in paints for energy saving. *Energy Build.* **2013**, *56*, 109–114. [CrossRef]
39. Azemati, A.; Rahimian Koloor, S.S.; Khorasanizadeh, H.; Sheikhzadeh, G.; Hadavand, B.S.; Eldessouki, M. Thermal evaluation of a room coated by thin urethane nanocomposite layer coating for energy-saving efficiency in building applications. *Case Stud. Therm. Eng.* **2023**, *43*, 102688. [CrossRef]

40. Sheikhzadeh, G.; Azemati, A.; Khorasanizadeh, H.; Hadavand, B.S.; Saraei, A. The effect of mineral micro particle in coating on energy consumption reduction and thermal comfort in a room with a radiation cooling panel in different climates. *Energy Build.* **2014**, *82*, 644–650. [CrossRef]
41. Marangoni, M.; Nait-Ali, B.; Smith, D.; Binhussain, M.; Colombo, P.; Bernardo, E. White sintered glass-ceramic tiles with improved thermal insulation properties for building applications. *J. Eur. Ceram. Soc.* **2017**, *37*, 1117–1125. [CrossRef]
42. Enríquez, E.; Fuertes, V.; Cabrera, M.; Seores, J.; Muñoz, D.; Fernández, J. New strategy to mitigate urban heat island effect: Energy saving by combining high albedo and low thermal diffusivity in glass ceramic materials. *Sol. Energy* **2017**, *149*, 114–124. [CrossRef]
43. Carlini, M.; Castellucci, S.; Ceccarelli, I.; Rotondo, M.; Mennuni, A. Study of a thermal dispersion in buildings and advantages of ceramic coatings for the reduction of energy expenditure. *Energy Rep.* **2020**, *6*, 116–128.
44. Ibrahim, M.; Bianco, L.; Ibrahim, O.; Wurtz, E. Low-emissivity coating coupled with aerogel-based plaster for walls' internal surface application in buildings: Energy saving potential based on thermal comfort assessment. *J. Build. Eng.* **2018**, *18*, 454–466. [CrossRef]
45. Triano-Juárez, J.; Macias-Melo, E.; Hernández-Pérez, I.; Aguilar-Castro, K.; Xamán, J. Thermal behavior of a phase change material in a building roof with and without reflective coating in a warm humid zone. *J. Build. Eng.* **2020**, *32*, 101648. [CrossRef]
46. Brito Filho, J.; Santos, T.O. Thermal analysis of roofs with thermal insulation layer and reflective coatings in subtropical and equatorial climate regions in Brazil. *Energy Build.* **2014**, *84*, 466–474. [CrossRef]
47. Arumugam, R.S.; Garg, V.; Ram, V.V.; Bhatia, A. Optimizing roof insulation for roofs with high albedo coating and radiant barriers in India. *J. Build. Eng.* **2015**, *2*, 52–58. [CrossRef]
48. Verma, R.; Rakshit, D. Comparison of reflective coating with other passive strategies: A climate based design and optimization study of building envelope. *Energy Build.* **2023**, *287*, 112973. [CrossRef]
49. Dong, C.; Zuo-ming, C.; Qiang, Z. Analysis of Several Test Methods about Heat Insulation Capabilities of Ceramic Thermal Barrier Coatings. *Phys. Procedia* **2013**, *50*, 248–252.
50. Antonaia, A.; Ascione, F.; Castaldo, A.; D'Angelo, A.; De Masi, R.F.; Ferrara, M.; Vanoli, G.P.; Vitiello, G. Cool materials for reducing summer energy consumptions in Mediterranean climate: In-lab experiments and numerical analysis of a new coating based on acrylic paint. *Appl. Therm. Eng.* **2016**, *102*, 91–107. [CrossRef]
51. Governatori, M.; Cedillo-González, E.; Manfredini, T.; Siligardi, C. Solar reflective properties of porcelain tiles for UHI mitigation: effect of highly reflective frits in the engobe's formulation. *Mater. Today Sustain.* **2022**, *20*, 100255. [CrossRef]
52. Tsoka, S.; Tsikaloudaki, A.; Theodosiou, T. Analyzing the ENVI-met microclimate model's performance and assessing cool materials and urban vegetation applications–A review. *Sustain. Cities Soc.* **2018**, *43*, 55–76. [CrossRef]
53. Di Giuseppe, E.; Pergolini, M.; Stazi, F. Numerical assessment of the impact of roof reflectivity and building envelope thermal transmittance on the UHI effect. *Energy Procedia* **2017**, *134*, 404–413.
54. Khare, V.R.; Vajpai, A.; Gupta, D. A big picture of urban heat island mitigation strategies and recommendation for India. *Urban Clim.* **2021**, *37*, 100845. [CrossRef]
55. Yang, J.; llamathy Mohan Kumar, D.; Pyrgou, A.; Chong, A.; Santamouris, M.; Kolokotsa, D.; Lee, S.E. Green and cool roofs' urban heat island mitigation potential in tropical climate. *Sol. Energy* **2018**, *173*, 597–609. [CrossRef]
56. Hayes, A.T.; Jandaghian, Z.; Lacasse, M.A.; Gaur, A.; Lu, H.; Laouadi, A.; Ge, H.; Wang, L. Nature-Based Solutions (NBSs) to Mitigate Urban Heat Island (UHI) Effects in Canadian Cities. *Buildings* **2022**, *12*, 925. [CrossRef]
57. Rosati, A.; Fedel, M.; Rossi, S. NIR reflective pigments for cool roof applications: A comprehensive review. *J. Clean. Prod.* **2021**, *313*, 127826. [CrossRef]
58. Blazejczyk, K.; Epstein, Y.; Jendritzky, G.; Staiger, H.; Tinz, B. Comparison of UTCI to selected thermal indices. *Int. J. Biometeorol.* **2012**, *56*, 515–535. [CrossRef] [PubMed]
59. Jendritzky, G.; de Dear, R.; Havenith, G. UTCI-Why another thermal index? *Int. J. Biometeorol.* **2012**, *56*, 421–428. [CrossRef]
60. Höppe, P. Different aspects of assessing indoor and outdoor thermal comfort. *Energy Build.* **2002**, *34*, 661–665. [CrossRef]
61. Wang, C.; Zhan, W.; Liu, Z.; Li, J.; Li, L.; Fu, P.; Huang, F.; Lai, J.; Chen, J.; Hong, F.; et al. Satellite-based mapping of the Universal Thermal Climate Index over the Yangtze River Delta urban agglomeration. *J. Clean. Prod.* **2020**, *277*, 123830. [CrossRef]
62. Ratti, C.; Raydan, D.; Steemers, K. Building form and environmental performance: Archetypes, analysis and an arid climate. *Energy Build.* **2003**, *35*, 49–59. [CrossRef]
63. Zhang, J.; Xu, L.; Shabunko, V.; Tay, S.E.R.; Sun, H.; Lau, S.S.Y.; Reindl, T. Impact of urban block typology on building solar potential and energy use efficiency in tropical high-density city. *Appl. Energy* **2019**, *240*, 513–533. [CrossRef]
64. Natanian, J.; Aleksandrowicz, O.; Auer, T. A parametric approach to optimizing urban form, energy balance and environmental quality: The case of Mediterranean districts. *Appl. Energy* **2019**, *254*, 113637. [CrossRef]
65. République Française. *Code de la Construction et de L'habitation*; 2013. Available online: https://www.google.com.hk/url?sa=t&rct=j&q=&esrc=s&source=web&cd=&ved=2ahUKEwj7q6S3hraBAxUIUGwGHamUBvgQFnoECBoQAQ&url=https%3A%2F%2Fcodes.droit.org%2FPDF%2FCode%2520de%2520la%2520construction%2520et%2520de%2520l%2527habitation.pdf&usg=AOvVaw2vsGtQJlf_paUXDxON6m4u&opi=89978449 (accessed on 12 July 2023).
66. Erell, E.; Pearlmutter, D.; Boneh, D.; Kutiel, P.B. Effect of high-albedo materials on pedestrian heat stress in urban street canyons. *Urban Clim.* **2014**, *10*, 367–386. [CrossRef]

67. Faragallah, R.N.; Ragheb, R.A. Evaluation of thermal comfort and urban heat island through cool paving materials using ENVI-Met. *Ain Shams Eng. J.* **2022**, *13*, 101609. [CrossRef]
68. Parison, S.; Hendel, M.; Royon, L. A statistical method for quantifying the field effects of urban heat island mitigation techniques. *Urban Clim.* **2020**, *33*, 100651. [CrossRef]
69. Hendel, M.; Gutierrez, P.; Colombert, M.; Diab, Y.; Royon, L. Measuring the effects of urban heat island mitigation techniques in the field: Application to the case of pavement-watering in Paris. *Urban Clim.* **2016**, *16*, 43–58. [CrossRef]